the temperature dependence of two of these components, the shear moduli C_{44} (T) and C_{55} (T). These moduli refer to shear over (001) planes in the [010] and [100] directions, respectively. The two sets of calculations [12, 13] disagree over these moduli, for example at $-196°C$, C_{44} is quoted [12] as 3.4×10^{10} dyn cm^{-2} and [13] as 4.5×10^{10} dyn cm^{-2}, while the calculated C_{55} are 1.2 and 2.3×10^{10} dyn cm^{-2}, respectively. At present there is no experimental value for either C_{44} or C_{55}. Now torsion about the c-axis of a single crystal of orthorhombic symmetry involves [14] terms in C_{44} as well as C_{55}, but torsion around D of the cylindrical specimen of Fig. 1 will involve only the crystal modulus C_{44} together with G_A, the shear modulus of amorphous polyethylene. Thus from the measured composite shear modulus, the known crystallinity and the estimated [15] value of G_A, a series model calculaton [16] would yield experimental values for C_{44} (T) to compare with the theoretical predictions.

Further work is under way in trying to improve the orientation; increasing the draw ratio to make a longer specimen will be the first step towards this, while it is also hoped to increase the transverse orientation function $f_{020,T}$ from 0.898 towards the value of 0.972 reported for a disc specimen of single crystal texture [17]. The results of the experiments outlined above will be published elsewhere.

Acknowledgements

The authors wish to thank Professor D. C. Phillips for the use of the diffractometer, Dr G. W. Groves for small angle X-ray photographs, and Drs N. G. McCrum and J. D. Campbell for useful discussions.

References

1. T. SETO and T. HARA, *Repts. Prog. Polymer Phys. Japan* **9** (1966) 207.
2. I. L. HAY and A. KELLER, *J. Mater. Sci.* **1** (1966) 41; **2** (1967) 538.
3. C. P. BUCKLEY, R. W. GRAY and N. G. MCCRUM, *J. Polymer Sci. B* **8** (1970) 341.
4. R. J. YOUNG, P. B. BOWDEN, J. M. RITCHIE and J. G. RIDER, *J. Mater. Sci.* **8** (1973) 23.
5. R. J. YOUNG and P. B. BOWDEN, *ibid* **8** (1973) 1177.
6. E. P. CHANG, R. W. GRAY and N. G. MCCRUM, *ibid* **8** (1973) 397.
7. C. R. DESPER and R. S. STEIN, *J. Appl. Phys.* **37** (1966) 3990.
8. G. W. GROVES and P. B. HIRSCH, *J. Mater. Sci.* **4** (1969) 929.
9. J. M. HUTCHINSON and N. G. MCCRUM, *Nature, Physical Science* **236** (1972) 115.
10. G. T. DAVIS, R. K. EBY and J. P. COLSON, *J. Appl. Phys.* **41** (1970) 4316.
11. F. C. STEHLING and L. MANDELKERN, *Macromolecules* **3** (1970) 242.
12. A. ODAJIMA and T. MAEDA, *J. Polymer Sci. C* **15** (1966) 55.
13. R. L. MCCULLOUGH and J. M. PETERSON, *J. Appl. Phys.* **44** (1973) 1224.
14. R. F. S. HEARMON, in "An Introduction to Applied Anisotropic Elasticity" (Oxford University Press, Oxford, 1961) p. 49.
15. R. W. GRAY and N. G. MCCRUM, *J. Polymer Sci. A2* **7** (1969) 1329.
16. C. P. BUCKLEY, R. W. GRAY and N. G. MCCRUM, *J. Polymer Sci. B* **7** (1969) 835.
17. R. W. GRAY and R. J. YOUNG, *J. Mater. Sci.* **9** (1974) 921.

Received 11 September
and accepted 25 October 1973

R. W. GRAY
Department of Electronics and Electrical Engineering, The University, Glasgow, UK

J. M. HUTCHINSON
Department of Engineering Science, Oxford University, Parks Road, Oxford, UK

J. F. MATHEWS
Department of Chemical Engineering, University of Saskatchewan, Saskatoon, Saskatchewan, Canada

Comments on "The equilibrium topography of sputtered amorphous solids"

Carter and his collaborators have reported a series of studies related to the equilibrium topography of sputtered amorphous solids [1-3]. In their recent work [3] the computer calculation has been devised to simulate the development of a general surface contour to the equilibrium condition. The purpose of this letter is to show that the two correction procedures described below should be introduced in their calculations and these corrections lead to the different

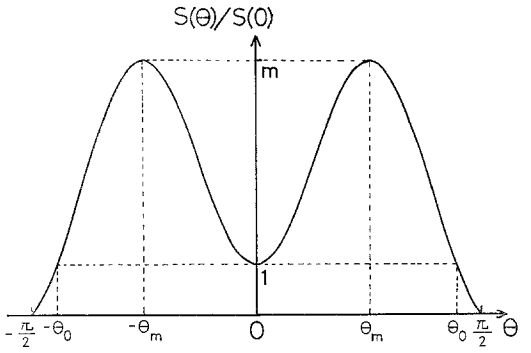

Figure 1 Sputtering yield $S(\theta)$ as a function of ion incidence θ.

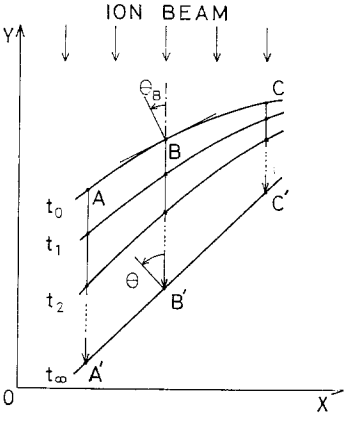

Figure 2 Erosion of a surface contour by sputtering.

developments of the surface topographies from their results.

In this treatment it is assumed that the changes of surface occur only as the result of atomic ejection and a sputtering yield is given as a function of angle of ion incidence. Hence, both the surface diffusion process and the redeposition of sputtered material are ignored. The basic equation of motion of the changing surface topography is given by [3]

$$\frac{\partial\theta}{\partial t} = -\frac{\Phi}{n}\frac{\partial S}{\partial\theta}\cos^2\theta\,\frac{\partial\theta}{\partial x}, \qquad (1)$$

where the surface contour is represented by a curve $y = f(x)$ and bombardment is by a uniform beam of Φ ions $\sec^{-1}$ in the negative y-direction. θ is the angle of incidence of the beam, with respect to the normal to any point on the target surface, i.e. $\tan\theta = \mathrm{d}y/\mathrm{d}x$, n is the atomic density of the target and S the sputtering yield (which is a function of θ of the form shown in Fig. 1, where $\pm\,\theta_m$ is the angle at which $S(\theta)$ reaches its maximum value, m). It is not generally possible to obtain the solution of Equation 1 to give a time-dependent variation of the contour.

For the convenience of the later discussion, we conjecture the development of the surface contour from Equation 1. Consider a concave downward surface bombarded in the negative y-direction as in Fig. 2, in which at any point B in the range from A to C on the surface ($x_A < x_B < x_C$), θ_B is initially always $\theta_m \geq \theta_A > \theta_B > \theta_C \geq 0$. Thus $(\partial S/\partial\theta) > 0$ and $(\partial\theta/\partial x) < 0$, $\partial\theta/\partial t$ is positive from Equation 1 and $S_A > S_B > S_C$, the curve tends towards a line at a certain angle θ to x-axis in the range from θ_A to θ_m. It is worthy of note that θ is not always equal to θ_m because the surface reaches the equilibrium slope once the surface contour becomes to a straight line, where $(\partial\theta/\partial t) = 0$ since $(\partial\theta/\partial x) = 0$. This result is tabulated in Table I, i.e. (a)-(2), with the similar results obtained under the other initial surface contours. The sketches of the developments of the surface topographies under the initial conditions (a) and (b) in Table I are shown in Figs. 3a and b, respectively. These developments are similar to those reached by Stewart and Thompson [4], and Carter *et al* [1].

For a more precise calculation of the development of the topography, the computer simulation is available to calculate the incremental value, Δy, of displacement of y-value at constant x on the surface during the lapse of time δt, and the new y-value is evaluated by subtracting this value from the original one. Since it is known that as $\delta t \to 0$, $\Delta y \to (\Phi/n)S\delta t$ [3], the new value of θ can be simply evaluated from the new slope of the surface by taking sampling points along x-axis. The present simulation has taken into account the correction procedure for the calculation of y to make the new values of θ satisfy the values of $\lim_{t\to\infty}\theta_B$ tabulated in Table I. For example, suppose a slight-concave upward surface as in Fig. 4, which satisfies $y_A < y_B < y_C$ and $0 \leq \theta_A < \theta_B < \theta_C \leq \theta_m$. Then this results in the relation $S_A < S_B < S_C$, i.e. $\Delta y_A < \Delta y_B < \Delta y_C$, but the new slope of the surface is not always satisfied by the condition described in Table I, i.e. $0 < \theta'_B < \theta_A$, if y' is directly derivated from $(y - \Delta y)$, as shown in Fig. 4. For the case of this example ($y'_B < y'_A < y'_C$), the new curve is chosen as $A' - B'' - C'$ in place of

TABLE I The slopes of equilibrium surface contours for the various initial conditions.

	$t = 0$		$t \to \infty$	
$\frac{\partial\theta}{\partial x}$	θ_B		$\frac{\partial S}{\partial\theta}$	$\theta = \lim_{t\to\infty} \theta_B$
(a) −	(1)	$\pi/2 \geq \theta_A > \theta_B > \theta_C \geq \theta_m$	(−)	$\theta_C \geq \theta \geq \theta_m$
	(2)	$\theta_m \geq \theta_A > \theta_B > \theta_C \geq 0$	(+)	$\theta_m \geq \theta \geq \theta_A$
	(3)	$0 \geq \theta_A > \theta_B > \theta_C \geq -\theta_m$	(−)	$\theta_C \geq \theta \geq -\theta_m$
	(4)	$-\theta_m \geq \theta_A > \theta_B > \theta_C \geqslant -\pi/2$	(+)	$-\theta_m \geq \theta \geq \theta_A$
(b) +	(1)	$\theta_m \leq \theta_A < \theta_B < \theta_C \leq \pi/2$	(−)	$\theta_C \leq \theta \leq \pi/2$
	(2)	$0 \leq \theta_A < \theta_B < \theta_C < \theta_m$	(+)	$0 \leq \theta \leq \theta_A$
	(3)	$-\theta_m \leq \theta_A < \theta_B < \theta_C < 0$	(−)	$\theta_C \leq \theta \leq 0$
	(4)	$-\pi/2 \leq \theta_A < \theta_B < \theta_C \leq -\theta_m$	(+)	$-\pi/2 \leq \theta \leq \theta_A$

(a) Concave downward surface; (b) concave upward surface.

$A' - B' - C'$ in the present calculation as a simple correction. Such an error is unavoidable so far as the numerical calculation is directly performed without introducing any additional conditions in the simulation. Another correction

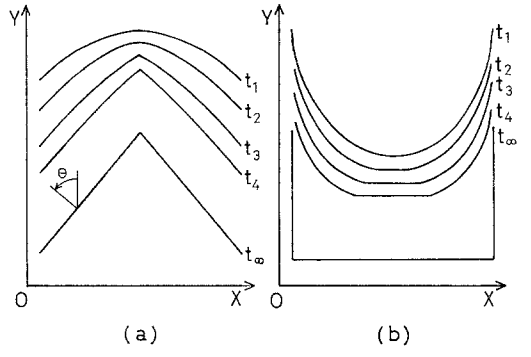

Figure 3 Developments of (a) a concave downward surface and (b) a concave upward surface.

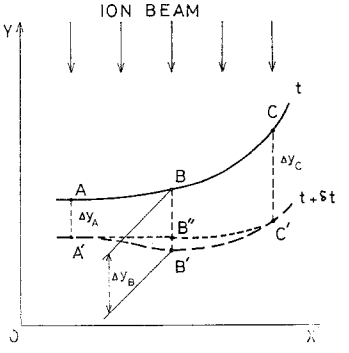

Figure 4 Illustration for the correction procedure used in the calculation of y.

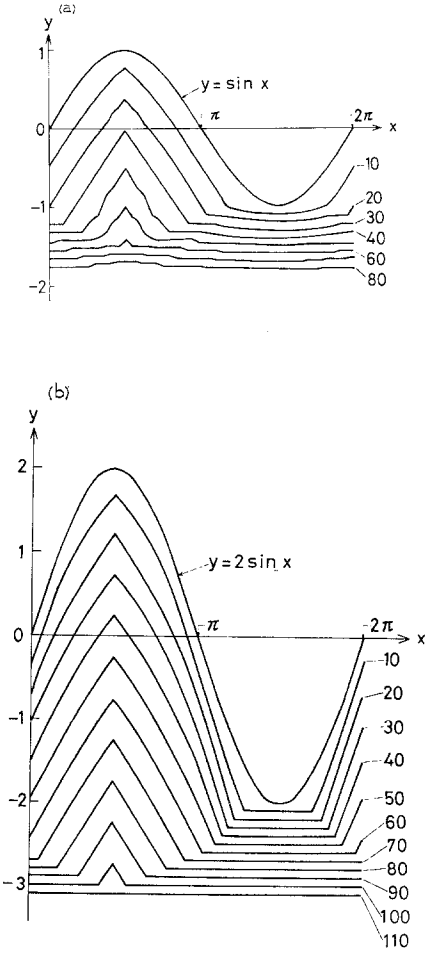

Figure 5 Changes of sinusoidal surfaces of (a) $y = \sin x$ and (b) $y = \sin x$. (The numbers on the contours indicate the number of steps calculated.)

was introduced by applying an averaging or weighting technique in the calculation of Δy, so that $(\Delta y_{i-1} + 2\Delta y_i + \Delta y_{i+1})/4$ was used instead of Δy_i. This correction is based upon the premise that the sputtering process is dictated by a collision cascade of finite dimensions and the target atoms are not always sputtered away one by one, so that the progress of the apical point, which is a discontinuity in $(\partial\theta/\partial x)$ in Equation 1, should be considered in relation to the motion of the surroundings. The necessity of the later correction has been already suggested by Carter *et al* [3].

Following Carter *et al* [3], the development of sinusoidal surfaces represented by $y = a \sin x$ are simulated in the present study by employing $S(\theta) = A \cos\theta + B\cos^2\theta + C\cos^4\theta$ as shown in Fig. 1. Figs. 5a and b show the changes of the typical surfaces of $a = 1$ and $a = 2$, respectively, under the same sputtering yield of $A = 3.4142$, $B = 12.7574$ and $C = -15.1716$, the curve of which has a maximum of $m = 5$ at $\theta_m = \pi/4$. Each figure shows that the triangle is formed in the early stage of sputtering, but at some points in the surface its development differs from that predicted by Carter *et al* [3]. One difference is that the sharp craters are not observed at the foot of the triangle. Another is that the slope of the triangular sections of the surface is nearly equal to θ_m, not θ_0 (the angle for which $S(\theta_0) = S(0)$) [3].

Consequently, these correction procedures mentioned above are considered to be necessary for the simulation of the development of real surfaces under ion bombardment.

References

1. M. J. NOBES, J. S. COLLIGON, and G. CARTER, *J. Mater. Sci.* **4** (1969) 730.
2. G. CARTER, J. S. COLLIGON, and M. J. NOBES, *ibid* **6** (1971) 115.
3. CRISTINA CATANA, J. S. COLLIGON, and G. CARTER, *ibid* **7** (1972) 467.
4. A. D. G. STEWART and M. W. THOMPSON, *ibid* **4** (1969) 56.

Received 8 October
and accepted 27 November 1973

T. ISHITANI
M. KATO
R. SHIMIZU
Department of Applied Physics, Osaka University, Suita, Japan

On the directional solidification of eutectic systems from the melt

A crystal growth method, allowing the growth from the melt of crystals having predetermined profiles, has recently been described in the literature [1, 2]. This technique has been called "edge-defined, film-fed, growth" (EFG) and involves the withdrawal of crystals from a thin liquid pool formed on the top planar surface of a shaping die. The liquid pool is fed by capillaries which extend down through the die into a liquid reservoir. The edge definition or crystal shaping is the result of the fulfilment of a contact angle requirement between the liquid and the die surface [3]. EFG has been investigated extensively by the growth of $\langle 0001 \rangle$ growth axis filamentary sapphire [2, 4, 5].

In recent years there has been a surge of interest in the field of directional solidification of eutectics with a view to their possible use in structural, electronic and optical applications. The present communication reports that EFG has been used to directionally solidify some ionic salt eutectic systems. The interphase relationship with growth speed has been determined, and several advantages which the method may offer over traditional directional solidification processes are suggested.

Details of the ribbon shaping die and crucible set-up, fabricated from nickel, have been described previously [6]. The eutectics chosen, LiF-CaF_2 and LiF-NaCl, were grown in an argon atmosphere. When the crucible and melt are heated to above the melting temperature of the eutectic mixture (prepared from 99.9% pure constituents), liquid rises to fill the feed slot of the die by capillary action. A small cleaved seed crystal of LiF, oriented so that $\langle 001 \rangle$ is along the growth axis, is lowered into contact with the melt in the capillary slot. After adjustment of melt temperature and seed withdrawal rate, the molten eutectic spreads across the top surface of the die and growth of a ribbon 0.6 cm wide × 0.15 cm thick is established.

Using this method several crystals were grown from each eutectic system at rates up to 40 cm h^{-1}. Withdrawal rate changes, together with melt temperature adjustments, were carried